International Journal of Pharmaceutics 361 (2008) 202–208

Contents lists available at ScienceDirect

International Journal of Pharmaceutics

journal homepage: www.elsevier.com/locate/ijpharm

Pharmaceutical Nanotechnology

Isolated swine heart ventricle perfusion model for implant assisted-magnetic drug targeting

Misael O. Avilés, Jan O. Mangual, Armin D. Ebner, James A. Ritter*

Department of Chemical Engineering, Swearingen Engineering Center, University of South Carolina, Columbia, SC 29208, USA

ARTICLE INFO

Article history:
Received 20 February 2008
Received in revised form 21 May 2008
Accepted 21 May 2008
Available online 23 June 2008

Keywords:
Implant assisted-magnetic drug targeting
MDT
Drug delivery
Drug targeting
High gradient magnetic separation
HGMS
Magnetic drug carrier particles
MDCPs
In vitro
Isolated organ perfusion

ABSTRACT

An isolated swine heart ventricle perfusion model was developed and used under physiologically relevant conditions to study implant assisted-magnetic drug targeting (IA-MDT). A stent coil was fabricated from a ferromagnetic SS 430 wire and used to capture 100-nm diameter magnetite particles that mimicked magnetic drug carrier particles (MDCPs). Four key cases were studied: (1) no stent and no magnet (control), (2) no magnet but with a stent, (3) no stent but with a magnet (traditional MDT), and (4) with a stent and a magnet (IA-MDT). When applied, the magnetic field was fixed at 0.125 T. The performance of the system was based on the capture efficiency (CE) of the magnetite nanoparticles. The experiments done in the absence of the magnetic field showed minimal retention of any nanoparticles whether the stent was present or not. The experiments done in the presence of the magnetic field showed a statistically significant increase in the retention of the nanoparticles, with a marked difference between the traditional and IA-MDT cases. Compared to the control case, in one case there was nearly an 11-fold increase in CE for the IA-MDT case compared to only a threefold increase in CE for the traditional MDT case. This enhanced performance by the IA-MDT case was typical of all the experiments. Histology images of the cross-section of the coronary artery revealed that the nanoparticles were captured mainly in the vicinity of the stent. Overall, the IA-MDT results from this work with actual tissue were very encouraging and similar to those obtained from other non-tissue and theoretical studies; but, they did point to the need for further studies of IA-MDT.

1. Introduction

The concept of magnetic drug targeting (MDT) has been around for over 30 years (Häfeli, 2004), and simply entails retaining specially designed magnetic drug carrier particles (MDCPs) at a specific site in the body using an externally applied magnetic field. However, due to magnetic forces generally being short ranged and underwhelming compared to hydrodynamic forces in the body, the targeted collection of such particles has met with limited success (Lübbe et al., 1999; Xu et al., 2005). As a result, the efficacies of the few clinical trials that have been carried out using this traditional MDT approach have fallen short of their expectation (Lübbe et al., 1999, 2001; Lemke et al., 2004). Research is still continuing with this traditional MDT approach (Alexiou et al., 2005; Ma et al., 2007; Seliger et al., 2007; Yoshida et al., 2007; Chertok et al., 2008); and in an attempt to overcome its shortcomings, the notion of using a ferromagnetic implant, in conjunction with the MDCPs and an external magnetic field, has recently been receiving considerable attention (Forbes et al., 2003, 2008; Chen et al., 2004, 2005; Iacob et al., 2004; Ritter et al., 2004; Avilés et al., 2005, 2007a,b, in press; Rosengart et al., 2005; Rotariu and Strachan, 2005; Yellen et al., 2005; Zheng et al., 2006; Fernandez-Pacheco et al., 2007). This new MDT technique is referred to as implant assisted (IA)-MDT.

IA-MDT exploits the fact that the magnetic force imparted on a particle (e.g., a MDCP) depends on both the magnitude (H) and the gradient of the magnetic field (∇H). It further exploits the fact that when a ferromagnetic element (e.g., a wire) is placed inside a magnetic field it becomes magnetized, which in turn increases both H and ∇H locally around the element. This idea is borrowed from the well-known principles of high gradient magnetic separation (HGMS) (Gerber, 1994). IA-MDT now simply entails implanting a ferromagnetic element at or near the target site and using this magnetized element to locally enhance the collection of the MDCPs there.

Several theoretical (Forbes et al., 2003; Chen et al., 2004, 2005; Iacob et al., 2004; Ritter et al., 2004; Avilés et al., 2005, 2007a; Rotariu and Strachan, 2005; Yellen et al., 2005), and some experimental *in vitro* (Yellen et al., 2005; Forbes et al., 2003; Avilés et al., 2007b, in press) and *in vivo* (Zheng et al., 2006; Fernandez-

* Corresponding author. Tel.: +1 803 777 3590; fax: +1 803 777 8265.
E-mail address: ritter@engr.sc.edu (J.A. Ritter).

0378-5173/$ – see front matter © 2008 Elsevier B.V. All rights reserved.
doi:10.1016/j.ijpharm.2008.05.027

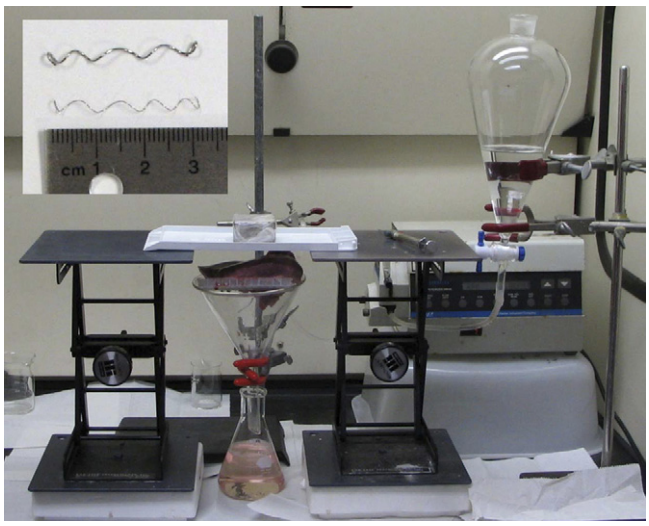

Fig. 1. Photograph of the isolated swine heart ventricle perfusion apparatus used in the *in vitro* experiments to study IA-MDT.

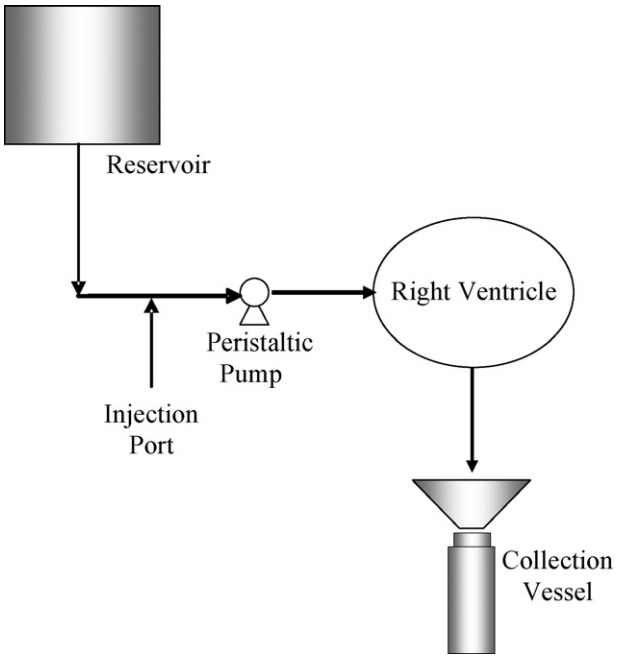

Fig. 2. Schematic of the isolated swine heart ventricle perfusion apparatus used in the *in vitro* experiments to study IA-MDT.

Pacheco et al., 2007; Forbes et al., 2008) studies have been carried out recently that emphatically show the advantage of IA-MDT over traditional MDT when using wires (Iacob et al., 2004; Ritter et al., 2004; Avilés et al., 2005; Rotariu and Strachan, 2005), stents (Chen et al., 2004, 2005; Yellen et al., 2005; Zheng et al., 2006; Avilés et al., 2007b; Forbes et al., 2008), and even seeds (Forbes et al., 2003; Avilés et al., 2007a, in press) as implants. As valuable as these studies have been in touting the fundamentals and applications of IA-MDT, only a paucity of them have encompassed the complexity of real biological systems (Zheng et al., 2006; Fernandez-Pacheco et al., 2007; Forbes et al., 2008), and none of them have accurately emulated the conditions normally found in the human body. Yet, these are the kinds of studies that are sorely needed to foster the further development of IA-MDT through clinical trials.

With this in mind, the objective of this work was to develop an isolated swine heart ventricle perfusion model to study the performance of IA-MDT under more realistic physiological conditions. A ferromagnetic stent was fabricated from coiled 430 SS wire and positioned inside the right coronary artery of an isolated swine heart, and 100-nm diameter magnetite particles were used to mimic MDCPs. The effects of several important parameters on the collection of these MDCPs were studied, including the fluid flow rate, stent wire diameter, and presence and absence of both the stent and the magnetic field. While a heart might not be considered as a typical organ for drug targeting applications, it was anticipated that the coronary artery and the capillary network of this isolated swine heart ventricle perfusion model would serve as an ideal platform to study IA-MDT applications in the circulatory system.

2. Experimental

Swine hearts averaging 300 g were obtained from a local meat processing plant. The hearts were received within 30 min of harvest, the right ventricle was dissected for further use, and the right coronary artery cannulated with a homemade cannula. 200 mL of saline solution (0.9%, w/v NaCl) containing 400 mg/L lidocaine (Sigma, USA) and 5000 units/L heparin (Sigma, USA) were infused through the artery to flush the blood from the tissue. The right ventricle was stored at 4 °C until needed.

Fig. 1 shows a photograph of the experimental apparatus used in the perfusion experiments. Fig. 2 depicts a simple schematic of this apparatus. A 1 L reservoir was connected to a peristaltic pump that was used to drive the saline/lidocaine/heparin solution through the cannulated coronary artery while controlling the average flow rate. The effluent was collected in a vessel and analyzed for iron using atomic absorption spectroscopy (AAS). When a magnetic field was applied, a single NdFeB permanent magnet (Dexter Magnetic Technology) was placed 2 cm away from the surface of the tissue, as shown in Fig. 1. At this distance, the applied magnetic field was 0.125 T, as measured using a Model 4048 Bell Gauss/Tesla meter. A SS 430 wire (Calfinewire), 5-cm long and either 200 or 500 μm in diameter, was used to create a 3-cm long by 3-mm diameter coiled stent with about 4 loops that was positioned inside the right coronary artery. A photograph of the two different diameter stents is shown in the insert of Fig. 1. The injection port was used to add

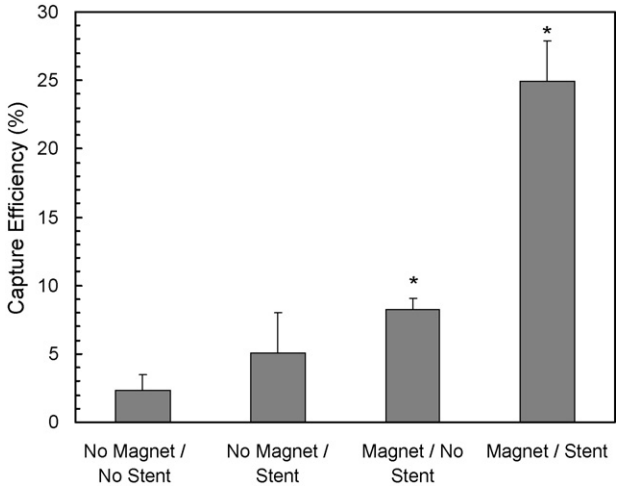

Fig. 3. Bar graphs of the capture efficiency (CE) of the 100 nm magnetite nanoparticles obtained from the four different experiments indicated. The flow rate was 40 mL/min, the stent wire diameter was 500 μm (when used), and the magnetic field strength was 0.125 T (when applied). The * indicates a statistically significant difference ($p < 0.05$) from the control case (no magnet and no stent).

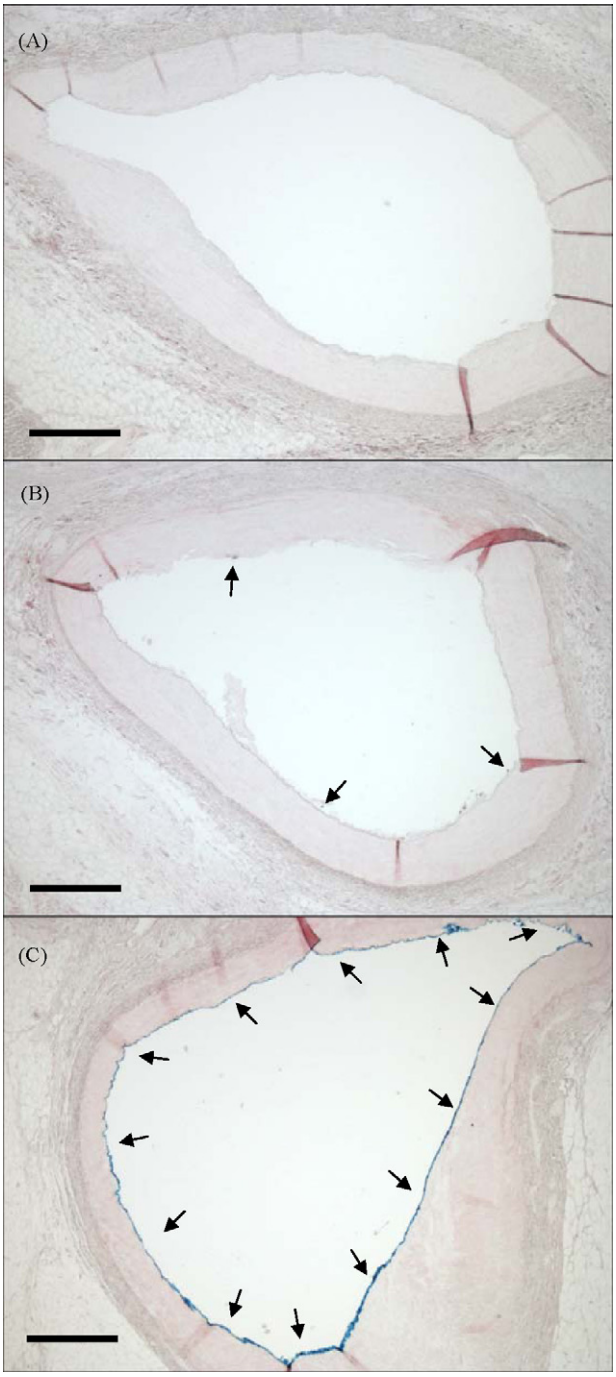

Fig. 4. Photomicrographs of the cross-section of the right coronary artery stained with Prussian Blue (for iron) and Nuclear Fast Red (for contrast). These histology images were obtained from three different experiments: (A) no magnet and no stent (control case), (B) no stent but with the magnet (traditional MDT case), and (C) with the magnet and the stent (IA-MDT case). The flow rate was 40 mL/min, the stent wire diameter was 500 μm (when used), and the magnetic field strength was 0.125 T (when applied). Blue regions (aided by the arrows) indicate the areas where iron, i.e., magnetite nanoparticles, is visible. Scale bar is 500 μm.

a suspension of 100-nm diameter magnetite particles (Chemicell, Germany) that were used to mimic MDCPs.

An experiment consisted of initially flowing 400 mL of the saline/lidocaine/heparin solution, followed by 200 mL of just saline solution through the cannulated artery. This solution entered the coronary artery, and flowed through it, branched arteries and heart tissue. Some of it exited the other end of the severed coronary

Fig. 5. Photograph of the partially segmented right coronary artery of the isolated swine heart exposing the stent and traces of the magnetite nanoparticles after an IA-MDT experiment. The flow rate was 40 mL/min, the stent wire diameter was 500 μm and the magnetic field strength was 0.125 T.

artery, some of it exited other small arteries and some of it seeped from all around the heart tissue. All of this effluent was collected and a sample was analyzed by AAS for iron. While keeping the flow of the saline solution constant, 0.5 mL of a 2.8 mg/mL MDCP suspension was then injected, and two 50 mL samples of effluent were collected and analyzed by AAS for iron. The system was flushed with 1 L of saline solution and a sample of the effluent was again collected and analyzed by AAS for iron. A magnet was then placed 2 cm away from the tissue and a second injection of 0.5 mL of a 2.8 mg/mL MDCP suspension was made. Again, two 50 mL samples of effluent were collected and analyzed by AAS for iron.

The performance of the system was characterized by the capture efficiency (CE), defined as the percentage of nanoparticles retained in the tissue, compared to those pumped through it. 2 mL aliquots from the samples were digested with 1 mL of concentrated nitric acid (Sigma, USA) at 105 °C for 1 h inside a vacuum oven, and analyzed using AAS for iron. Tissue samples were fixed in 10% buffered formalin and stained with Prussian Blue (Polysciences), a specific stain for iron, and with Nuclear Fast Red (Polysciences), a contrast stain.

The first set of experiments consisted of using heart tissue without the stent, performing the experiments initially without the magnet, and then using the same heart with the magnet in place. A second set of experiments consisted of carrying out the same procedure, but with the stent implanted inside the right coronary artery of the heart tissue. Average flow rates of 20, 40 and 80 mL/min were used, which corresponded to average artery velocities of approximately 5, 10 and 20 cm/s with the 3-mm diameter coiled stent in place.

All experiments were done in triplicate with different heart tissue samples for statistical analysis. The average from the three runs was computed and presented around one standard deviation. Statistical analysis was done using a *T*-test analysis with $p < 0.05$ found to be significantly different.

3. Results and discussion

A series of IA-MDT experiments were carried out with the isolated swine heart right ventricle perfusion model to study the feasibility of retaining MDCPs within this kind of vasculature. The notion was to demonstrate that inside of actual tissue, using conditions normally found in the human body, a significant number

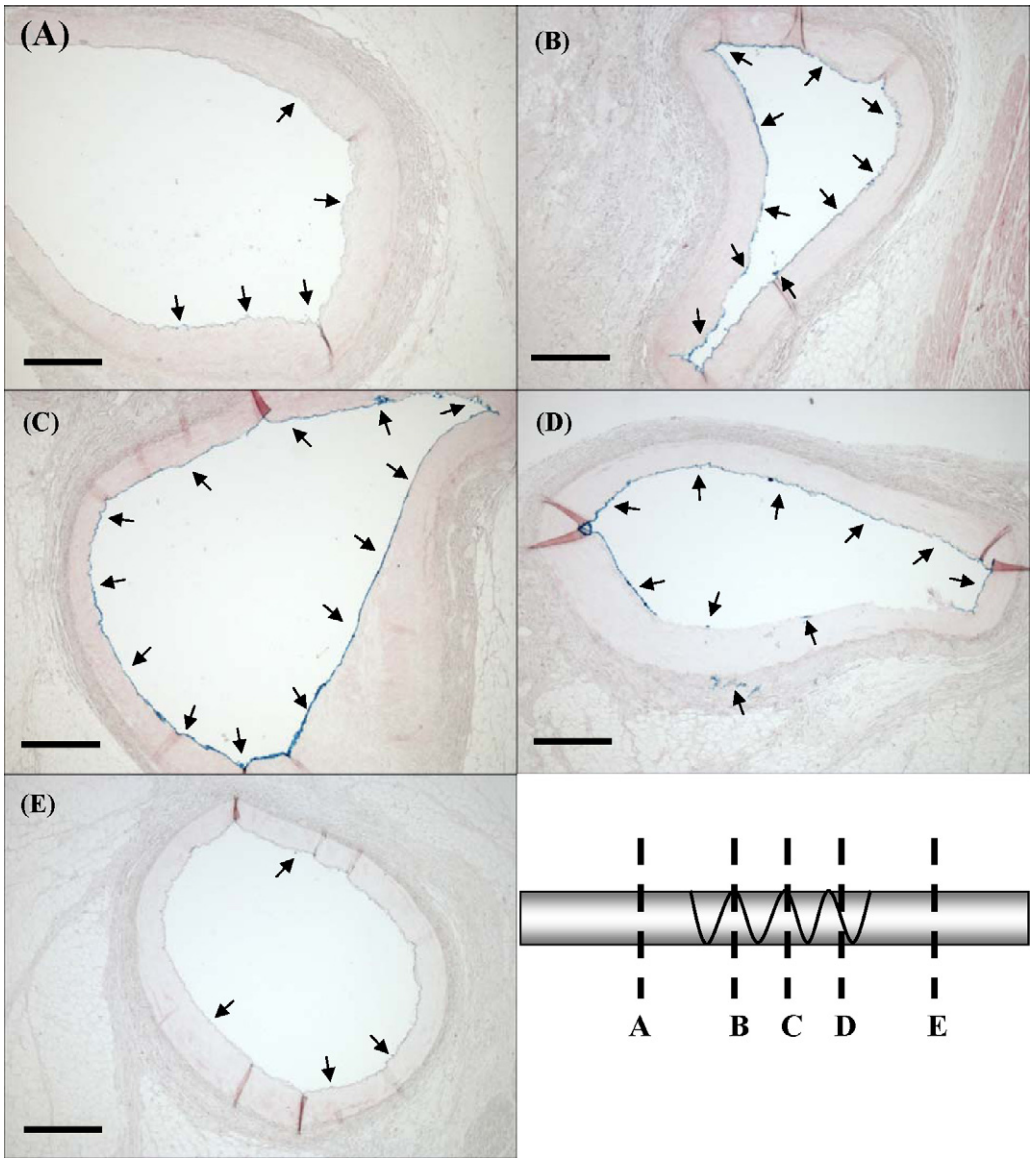

Fig. 6. Photomicrographs of the cross-section of the right coronary artery stained with Prussian Blue (for iron) and Nuclear Fast Red (for contrast). These histology images were obtained from five different locations along the artery after an IA-MDT experiment: (A) before the stent, (B) at the beginning of the stent, (C) at the middle of the stent, (D) at the end of the stent, and (E) after the stent. The flow rate was 40 mL/min, the stent wire diameter was 500 μm, and the magnetic field strength was 0.125 T. Blue regions (aided by the arrows) indicate the areas where iron, i.e., magnetite nanoparticles, is visible. Scale bar is 500 μm.

of magnetite nanoparticles would be captured, just like in previous non-tissue studies (Avilés et al., 2007b). Two parameters were investigated, i.e., the fluid flow rate and the diameter of the stent wire, in the presence and absence of the stent and in the presence and absence of the applied magnetic field. Two of these four possible cases represented the traditional and implant assisted MDT approaches, while the other two represented non-magnetic situations, with one of them being the control case (no magnet and no stent). The results are shown in Figs. 3–8.

Fig. 3 shows a plot of the capture efficiency of the MDCPs for the four different situations, i.e. (1) with no magnet and no stent (control case), (2) with no magnet but with a stent, (3) with no stent but with a magnet, and (4) with both the magnet and the stent. In all cases, the stents were made from the 500-μm diameter wire, and the flow rate was set at 40 mL/min. First and foremost, in the control case the capture efficiency (CE) of the magnetite nanoparticles in the tissue averaged less than 3%. Even when the stent was put in place without the magnet, the CEs were still quite low, averaging only about 5% and exhibiting no statistical difference from the control case. These results were very important because they demonstrated conclusively that the nanoparticles were unobstructed while passing through the artery and capillary tissue of the isolated swine heart. In contrast, when the magnet was used without the stent being present, i.e., the traditional MDT scenario, the CE increased to just over 8%, which was still quite low but statistically different from the control case. Although the applied magnetic field clearly caused a slight increase in the retention of the nanoparticles within the tissue, this result confirmed the less than adequate performance typically produced by the traditional MDT approach. However, when the stent and the magnetic field were both present, i.e., the IA-MDT scenario, the CE increased to 25%. This was a significant increase in the CE compared to any of the other cases. In fact, the CE increased by a factor of three compared to the magnet alone case and by a factor of nearly 11 compared to the control case. These results were very encouraging as they unmistakably showed that the presence of the implant significantly increased the capture of

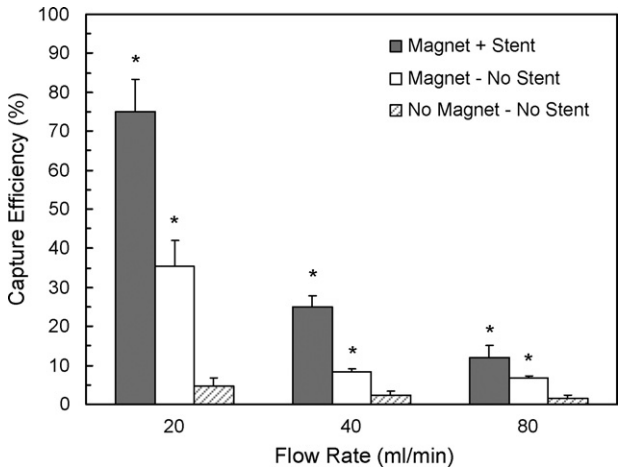

Fig. 7. Bar graphs of the capture efficiency (CE) of the 100 nm magnetite nanoparticles obtained for different flow rates through the coronary artery for the three different experiments indicated. The stent wire diameter was 500 μm (when used), and the magnetic field strength was 0.125 T (when applied). The * indicates a statistically significant difference ($p < 0.05$) from the control case (no magnet and no stent).

the nanoparticles inside the tissue under conditions that mimicked the human body.

More confirmation of the effectiveness of the implant is provided in photomicrographs of the cross-section of the coronary artery shown in Fig. 4. Three cases were examined, i.e. (A) with no stent and no magnet (control case), (B) with no stent but with the magnet (traditional MDT case), and (C) with both the stent and the magnet (IA-MDT case). For this study, the 500-μm diameter stent wire was used along with a flow rate of 40 mL/min. All tissue samples were obtained from the center of the artery where the stent and the magnet were located, if present. The presence of iron, which was stained blue, revealed where the magnetite nanoparticles were located; the tissue was stained red. The control case showed that essentially no nanoparticles were collected within the lumen of the artery. The traditional MDT case showed that some but not many nanoparticles were collected on the inner lumen of the artery. In contrast, the IA-MDT case showed that a significant number of particles had collected along the entire inner lumen of the artery, forming a continuous layer completely around the circumference. These results all agreed with the results shown in Fig. 3 and demonstrated that the presence of the implant in the artery caused the localized capture of a significant number of magnetite nanoparticles near the implant.

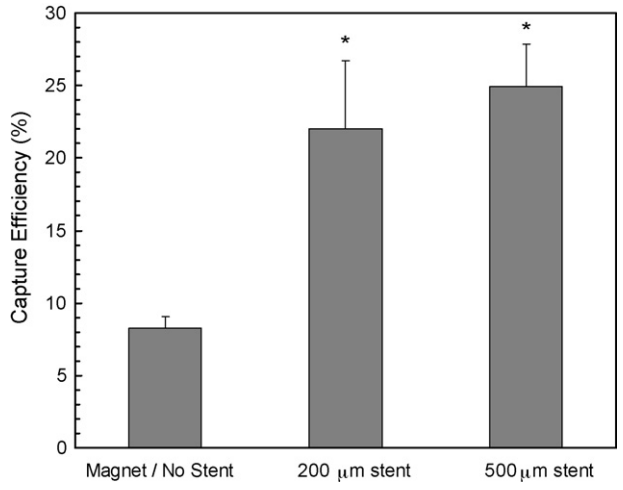

Fig. 8. Bar graphs of the capture efficiency (CE) of the 100 nm magnetite nanoparticles obtained for the different stent wire diameters indicated and the traditional MDT case (no stent but with a magnet). The flow rate was 40 mL/min and the magnetic field strength was 0.125 T. The * indicates a statistically significant difference ($p < 0.05$) from the control case (no magnet and no stent).

To show that the nanoparticles were indeed collected in the tissue in the general vicinity of the implant, a photograph of the swine heart left ventricle was taken after segmenting part of the artery to expose the stent after an IA-MDT experiment was finished. This photograph is shown in Fig. 5. The flow rate for this experiment was 40 mL/min and the stent wire diameter was 500 μm. The magnetite particles were observed very clearly around the stent but not before the stent in the excised artery. For the same purpose, tissue samples were also taken along the length of the right coronary artery of a heart just after it was tested with the stent and magnet in place (IA-MDT case). Fig. 6 shows the resulting photomicrographs of stained artery cross-sections at five different locations: (A) before the stent, (B) at the beginning of the stent, (C) at the center of the stent, (D) at the end of the stent, and (E) after the stent. It was evident that the majority of the nanoparticles were located in the lumen of the artery of only those images taken along the stent, as observed from Fig. 6B–D. A layer of nanoparticles (stained blue) was again covering the entire lumen of the artery at those locations. Although the tissue samples taken before and after the stent (Fig. 6A and E) contained some nanoparticles in the lumen of the artery, the amount was minimal compared to the other cases. These results convincingly demonstrated that the stent not only increased the amount of nanoparticles captured, but it also localized, i.e., concentrated, them at a specific location in the vicinity of the stent.

The effect of the fluid flow rate through the artery on the CE of the MDCP nanoparticles was also studied because the blood velocity varies widely depending on the specific blood vessel and site. Fig. 7 shows this effect for flows rates of 20, 40, and 80 mL/min, which encompass conditions that are found in many small arteries, arterioles, and veins. Three cases were studied: the control case, the traditional MDT case and the IA-MDT case with the stent made from the 500 μm wire. In all three scenarios an increase in the flow rate had a negative effect on the CE of the nanoparticles. These results exhibited the same trends as those reported elsewhere (Avilés et al., 2007b) and were expected since for a particle to be magnetically captured the magnetic force must overcome the hydrodynamic force, which increases with increasing flow rate. Nevertheless, when the magnetic field was applied the resulting CEs were always statistically higher than those obtained from the control case, especially for the IA-MDT case. In fact, for that case, more than 75% of the nanoparticles were retained at a flow of 20 mL/min, which was more than twice that obtained with the magnet alone, and more than 16 times that achieved in the control case. Similar, marked increases in the CEs were observed at the other two flow rates, as well. These results clearly showed the vital role-played by the stent in the collection of a significant number of nanoparticles, especially at low flow rates like those found in small arteries, arterioles and veins. However, they also began to illuminate some of the challenging aspects associated with IA-MDT especially when trying to capture such small magnetic nanoparticles under relatively high flow rates that are readily found in larger arteries.

The diameter of the stent wire on the CE of the MDCP nanoparticles was also studied because previous studies have shown this to be an important IA-MDT design parameter (Chen et al., 2005). For this purpose, a second stent was made from a 200-μm diameter wire. It had the same number of coils, coil diameter, and length as the 500-μm diameter stent, as shown in the insert of Fig. 1. In terms of the CE of the MDCP nanoparticles, Fig. 8 compares the IA-

MDT results obtained with both diameter wires to the traditional MDT case (no stent) at a flow rate of 40 mL/min. The performance obtained from either wire was significantly better than that from the traditional MDT case, as expected from previous results. However, there was no statistical difference between the CEs obtained from the 200 to 500 μm diameters stents; although, on average, the larger wire did perform slightly better. According to a theoretical study (Chen et al., 2005), the CE should have increased with increasing stent wire diameter for the same size blood vessel, but only slightly for such small particles. Although on average this was true, statistically there was no difference, even though the stent wire diameters differed by 2.5 times. This result suggested that a much broader parameter study needs to be carried out. This result also illustrated that the stent wire diameter could very considerably in size without having much effect of the collection of the MDCPs, at least within the narrow range of blood vessel and stent wire diameters studied here.

4. Conclusions

An isolated swine heart ventricle perfusion model was developed and used to study implant assisted-magnetic drug targeting (IA-MDT). A 3-cm long by 3-mm diameter stent coil with approximately 4 loops was fabricated from a 5-cm long piece of ferromagnetic SS 430 wire and used to capture 100 nm diameter magnetite particles that mimicked actual magnetic drug carrier particles (MDCPs). The notion was to conduct a series of experiments using physiological tissue and conditions to further demonstrate the feasibility of IA-MDT.

Four key cases were studied: (1) no stent and no magnet (control case), (2) no magnet but with a stent, (3) no stent but with a magnet (traditional MDT case), and (4) with a stent and a magnet (IA-MDT case). When applied, the magnetic field was fixed at 0.125 T. The fluid flow (20, 40, and 80 mL/min) through the right coronary artery and the wire stent diameter (200 and 500 μm) were also studied. The performance of the system was based on the capture efficiency (CE) of the magnetite nanoparticles, which was defined as the percentage of particles retained in the tissue that entered the system.

The experiments done in the absence of the magnetic field showed minimal retention of any nanoparticles whether the stent was present or not. In contrast, the experiments done in the presence of the magnetic field showed a statistically significant increase in the retention of the nanoparticles, with a marked difference between the traditional and IA-MDT cases. Compared to the control case, in one set of experiments there was nearly an 11-fold increase in the CE for the IA-MDT case compared to only a threefold increase in the CE for the traditional MDT case. Under similar conditions, this enhanced performance by the IA-MDT case was typical of all the experiments. Histology images of the cross-section of the coronary artery revealed that the nanoparticles were captured mainly in the vicinity of the stent, an important observation.

It was found that the CE decreased with an increase in the flow rate. In contrast, it was also found that the CE statistically did not change with an increase in the stent wire diameter; although, on average it increased slightly. Based on previous theoretical studies, the former result was expected and understood, while the latter result was not expected and needs further study.

Overall, this first of its kind *in vitro* study with an isolated swine heart ventricle perfusion model clearly demonstrated the significant advantage afforded by using a ferromagnetic implant with MDT. It was also encouraging that the IA-MDT results from this work with actual tissue were similar to those obtained from other non-tissue and theoretical studies. However, they did point to the need for further studies of IA-MDT using the isolated swine heart ventricle perfusion model developed in this work.

Acknowledgements

Research support provided by the following agencies and institutions was greatly appreciated: NSF under grant Nos. CTS-0314157 and CTS-0508391, the Sloan Foundation Graduate Research Fellowship provided to MOA and JOM, the Ford Foundation Graduate Research Fellowship provided to MOA, the NSF K-12 Graduate Fellowship provided to JOM, and the USC NanoCenter.

References

Alexiou, C., Jurgons, R., Schmid, R., Hilpert, A., Bergemann, C., Parak, F., Iro, H., 2005. In vitro and in vivo investigations of targeted chemotherapy with magnetic nanoparticles. J. Mag. Mag. Mater. 293, 389–393.

Avilés, M.O., Ebner, A.D., Chen, H., Rosengart, A.J., Kaminski, M.D., Ritter, J.A., 2005. Theoretical analysis of a transdermal ferromagnetic implant for retention of magnetic drug carrier particles. J. Mag. Mag. Mater. 293, 605–615.

Avilés, M.O., Ebner, A.D., Ritter, J.A., 2007a. Ferromagnetic seeding for the magnetic targeting of drugs and radiation in capillary beds. J. Mag. Mag. Mater. 310, 131–144.

Avilés, M.O., Ebner, A.D., Ritter, J.A., 2007b. In vitro study of ferromagnetic stents for implant assisted-magnetic drug targeting. J. Mag. Mag. Mater. 311, 306–311.

Avilés, M.O., Ebner, A.D., Ritter, J.A., *In vitro* study of magnetic particle seeding for implant assisted-magnetic drug targeting. J. Mag. Mag. Mater, in press.

Chen, H., Ebner, A.D., Rosengart, A.J., Kaminski, M.D., Ritter, J.A., 2004. Analysis of magnetic drug carrier particle capture by a magnetizable intravascular stent. 1. Parametric study with single wire correlation. J. Mag. Mag. Mater. 284, 181–194.

Chen, H., Ebner, A.D., Rosengart, A.J., Kaminski, M.D., Ritter, J.A., 2005. Analysis of magnetic drug carrier particle capture by a magnetizable intravascular stent. 2. Parametric study with multi-wire two-dimensional model. J. Mag. Mag. Mater. 293, 616–632.

Chertok, B., Moffat, B.A., David, A.E., Yu, F., Bergemann, C., Ross, B.D., Yang, V.C., 2008. Iron oxide nanoparticles as a drug delivery vehicle for MRI monitored magnetic targeting of brain tumors. Biomaterials 29, 487–496.

Fernandez-Pacheco, R., Marquina, C., Valdivia, J.G., Gutierrez, M., Romero, M.S., Cornudella, R., Laborda, A., Vitoria, A., Higuera, T., Garcia, A., Garcia de Jalon, J.A., Ibarra, M.R., 2007. Magnetic nanoparticles for local drug delivery using magnetic implants. J. Mag. Mag. Mater. 311, 318–322.

Forbes, Z.G., Yellen, B.B., Barbee, K.A., Friedman, G., 2003. An approach to targeted drug delivery based on uniform magnetic fields. IEEE Trans. Mag. 39, 3372–3377.

Forbes, Z.G., Yellen, B.B., Halverson, D.S., Fridman, G., Barbee, K.A., Friedman, G., 2008. Validation of high gradient magnetic field based drug delivery to magnetizable implants. IEEE Trans. Biomed. Eng. 55, 643–649.

Gerber, R., 1994. Applied magnetism. In: Gerber, R., Wright, C.D., Asti, G. (Eds.), NATO ASI Series, Series E: Applied Sciences, 253. Kluwer Academic Publishers, Dordrecht.

Häfeli, U.O., 2004. Magnetically modulated therapeutic systems. Int. J. Pharm. 277, 19–24.

Iacob, G., Rotariu, O., Chiriac, H., 2004. A possibility for local targeting of magnetic carriers. J. Optoelec. Adv. Mater. 6, 713–717.

Lemke, A.J., Senfft von Pilsach, M.-I., Lübbe, A., Bergermann, C., Riess, H., Felix, R., 2004. MRI after magnetic drug targeting in patients with advance solid malignant tumors. Eur. Radiol. 14, 1949–1955.

Lübbe, A.S., Bergemann, C., Brock, J., McClure, D.G., 1999. Physiological aspects in magnetic drug-targeting. J. Mag. Mag. Mater. 194, 149–155.

Lübbe, A.S., Alexiou, C., Bergemann, C., 2001. Clinical applications of magnetic drug targeting. J. Surg. Res. 95, 200–206.

Ma, Y.-H., Hsu, Y.-W., Chang, Y.-J., Hua, M.-Y., Chen, J.-P., Wu, T., 2007. Intra-arterial application of magnetic nanoparticles for targeted thrombolytic therapy: a rat embolic model. J. Mag. Mag. Mater. 311, 342–346.

Ritter, J.A., Ebner, A.D., Daniel, K.D., Stewart, K.L., 2004. Application of high gradient magnetic separation principles to magnetic drug targeting. J. Mag. Mag. Mater. 280, 184–201.

Rosengart, A.J., Kaminski, M.D., Chen, H., Caviness, P.L., Ebner, A.D., Ritter, J.A., 2005. Magnetizable implants and functionalized magnetic carriers: a novel approach for noninvasive yet targeted drug delivery. J. Mag. Mag. Mater. 293, 633–638.

Rotariu, O., Strachan, N.J.C., 2005. Modeling magnetic carrier particle targeting in the tumor microvasculature for cancer treatment. J. Mag. Mag. Mater. 293, 639–646.

Seliger, C., Jurgons, R., Wiekhorst, F., Eberbeck, D., Trahms, L., Iro, H., Alexiou, C., 2007. In vitro investigation of the behavior of magnetic particles by a circulating artery model. J. Mag. Mag. Mater. 311, 358–362.

Xu, H., Song, T., Bao, X., Hu, L., 2005. Site-directed research of magnetic nanoparticles in magnetic drug targeting. J. Mag. Mag. Mater. 293, 514–519.

Yellen, B.B., Forbes, Z.G., Halverson, D.S., Fridman, G., Barbee, K.A., Chorny, M., Levy, R., Friedman, G., 2005. Targeted drug delivery to magnetic implants for therapeutic applications. J. Mag. Mag. Mater. 293, 647–654.

Yoshida, Y., Fukui, S., Fujimoto, S., Mishima, F., Takeda, S., Izumi, Y., Ohtani, S., Fujitani, Y., Nishijima, S., 2007. Ex vivo investigation of magnetically targeted drug delivery system. J. Mag. Mag. Mater. 310, 2880–2882.

Zheng, J., Wang, J., Tang, T., Li, G., Cheng, H., Zou, S., 2006. Experimental study on magnetic drug targeting in treating cholangiocarcinoma based on internal magnetic fields. Chin. German J. Clin. Oncol. 5, 336–338.